

ON THE PRESENCE OF WATER AND GLOBAL CIRCULATION IN THE TRANSITING PLANET HD 189733B

TRAVIS S. BARMAN

Lowell Observatory, 1400 W. Mars Hill Rd., Flagstaff, AZ 86001

Email: barman@lowell.edu

Received 2007 October 26; accepted 2008 February 5

ABSTRACT

Detailed models are compared to recent infrared observations of the nearby extrasolar planet, HD 189733b. It is demonstrated that atmospheric water is present and that the planet's day side has a non-isothermal structure down to gas pressures of ~ 0.1 bars. Furthermore, model spectra with different amounts of CO are compared to the observations and an atmosphere absent of CO is excluded at roughly 2-sigma. Constraining the CO concentration beyond that is unfortunately not possible with the current *Spitzer* photometry. However, radically enhanced (or depleted) metal abundances are unlikely and the basic composition of this planet is probably similar to that of its host star. When combined with *Spitzer* observations, a recent ground-based upper limit for the *K*-band day side flux allows one to estimate the day-to-night energy redistribution efficiency to be $\sim 43\%$.

Subject headings: planetary atmospheres - extrasolar planets

1. INTRODUCTION

Hundreds of extrasolar planets have now been discovered along with over a dozen transiting systems. Despite the rapid pace of discovery, many important questions remain unanswered, especially concerning the transiting giant planets (hot-Jupiters). How efficiently is incident stellar energy absorbed by the day side redistributed to the night side? Do hot-Jupiters have atmospheres with enhanced metal abundances relative their host star? And under what conditions (and depths) are the day side atmospheric temperature structures isothermal? Fortunately, for the handful of nearby transiting planets, direct flux measurements have been obtained using the *Spitzer Space Telescope*. Fluxes provide a direct look into a planet's depth-dependent atmospheric conditions and perhaps hold the answers to some of these questions.

HD 189733b, is the closest known jovian-mass transiting planet (Bouchy et al. 2005), and flux measurements of its day side are available across a wide range of infrared wavelengths along with a recent measurement of the planet's night side at $8\ \mu\text{m}$ (Deming et al. 2006; Grillmair et al. 2007; Charbonneau et al. 2008; Knutson et al. 2007). HD 189733b is expected to have photospheric temperatures in the 1000 to 1500K range on its day side maintained by the large amount of incident stellar flux. At just 20 pc away from Earth, this planet is a valuable test case for atmospheric dynamics and chemical enrichment by accretion of extrasolar comets and asteroids.

In this Letter atmospheric models are compared to recent IR observations of HD 189733b to infer some of its basic photospheric properties. The concentrations of important molecules (e.g., water and CO) are discussed along with the day-to-night energy redistribution by depth-dependent horizontal circulations.

2. ECLIPSE DEPTHS AND SPECTRA

As a transiting planet passes behind its host star a small but measurable drop in infrared flux occurs as the planet's day side contribution disappears. A few hours later, the planet reappears from behind the host star and

the total system flux returns to its previous value. The change in flux during this secondary eclipse provides a precise measurement of the day side planet-star flux density ratio ($\epsilon_\lambda = \left[\frac{R_p^2 F_p}{R_\star^2 F_\star} \right]_\lambda$, where $R_{p,\star}$ are the planet and star radii) at a given wavelength. Since even heavily irradiated planets are much cooler than their host star, their peak flux emerges at a significantly longer wavelength (λ_p^{max}) than it does for the host star causing ϵ_λ to rise toward longer wavelengths and making secondary eclipse observations more practical at $\lambda \gtrsim \lambda_p^{max}$. Regardless of the detailed absorption features in the two spectra, ϵ_λ falls rapidly from the infrared to the optical as a result of the steep rise of the stellar spectrum and, consequently, the deepest eclipse measurements made with *Spitzer* are generally where the planet flux density is small.

Secondary eclipses of HD 189733 have been observed photometrically with *Spitzer* at 3.6, 4.5, 5.8, 8.0, 16 and $24\ \mu\text{m}$ (Deming et al. 2006; Charbonneau et al. 2008; Knutson et al. 2007). A secondary eclipse has also been observed spectroscopically from 7.5 to $15\ \mu\text{m}$ (Grillmair et al. 2007). Figure 1 shows all of the day side *Spitzer* secondary eclipse photometry for HD 189733 compared to a synthetic ϵ_λ spectrum produced by dividing a synthetic planet spectrum by a synthetic stellar spectrum (optimized for the K-type stellar host). The ϵ_λ spectrum has also been scaled by the planet-star surface areas determined from transit observations (Bouchy et al. 2005).

Given that ϵ_λ emphasizes the faintest portions of the planet's spectrum, comparing actual planet fluxes to model spectra is more revealing. The observed fluxes shown in Fig. 2 were calculated using the out-of-eclipse stellar fluxes and the definition of ϵ_λ above. As can be seen, the planet's spectrum peaks at $\sim 3.6\ \mu\text{m}$ – far from the deepest *Spitzer* eclipse depth. Also, while ϵ_λ is nearly flat from 3.6 to $4.5\ \mu\text{m}$, the individual planet spectrum is quite steep across this wavelength range.

Overall, the observations agree fairly well with the model shown in Fig. 2 (same model in Fig. 1). The standard model includes a solar abundance composition in

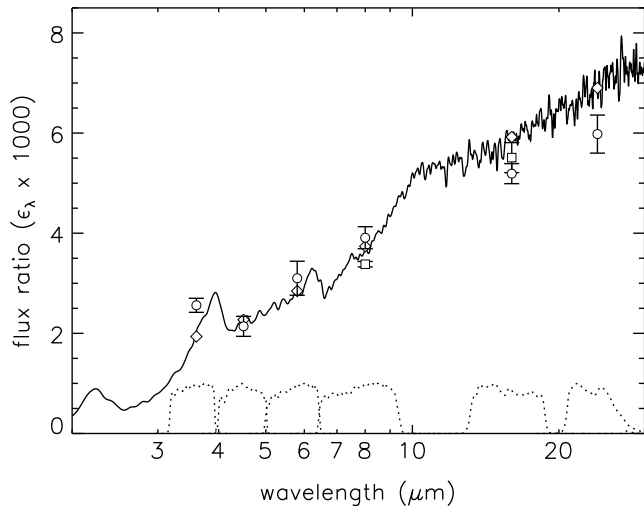


FIG. 1.— Model planet-star flux density ratios (ϵ_λ) assuming no energy is redistributed to the night side. White circles are the Charbonneau et al. (2008) *Spitzer* secondary eclipse measurements with $1-\sigma$ error-bars. White boxes are additional 8.0 and 16 μm eclipse values (Deming et al. 2006; Knutson et al. 2007). White diamonds are the model values integrated across the *Spitzer* instrumental response curves, indicated by dotted lines.

chemical equilibrium and irradiation following the methods described in Barman et al. (2001, 2005). Furthermore, this model assumes no redistribution of absorbed stellar flux from the day side to the night side and, hence, implies a very cold night side. Interestingly, zero energy redistribution to the night side is at odds with recent 8 μm observations indicating a warm night side photosphere (Knutson et al. 2007). Also, Burrows et al. (2006) found that their full-redistribution model (50% of the incident energy carried to the night side) is in good agreement with the Deming et al. (2006) 16 μm *Spitzer* observation. However, the Burrows et al. model predicts stronger absorption across the central two IRAC bands than is observed.

3. EVIDENCE FOR WATER AND CO

For the temperatures and pressures expected in the atmospheres of irradiated giant planets, models predict that H_2O should be the third or fourth most abundant gas-phase molecule. With its broad absorption features across the IR, H_2O plays an important role in sculpting a giant planet's emergent spectrum and temperature structure. Therefore, measuring the water abundance is an important step toward understanding the planet's overall chemistry and structure.

Given that basic predictions of hot-Jupiters include a copious water supply, the first spectra of hot-Jupiters were somewhat surprising in that no water absorption was detected. These ϵ_λ spectra turned out to be fairly flat from 7.5 to 11 μm which was interpreted as an absence of water absorption in the planet's spectrum (Grillmair et al. 2007; Richardson et al. 2007). A few months after the IRS spectra were published, evidence for water absorption in the atmosphere of HD 209458b was identified (Barman 2007) and a similar claim followed for HD 189733b (Tinetti et al. 2007). These water

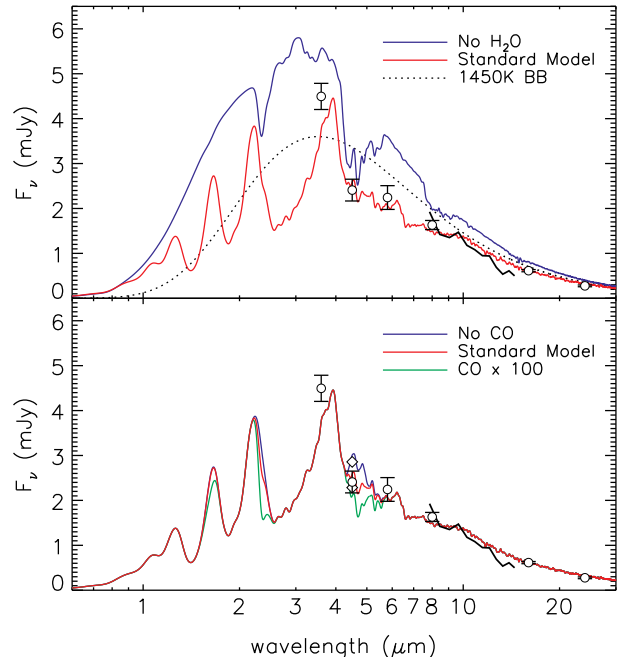


FIG. 2.— *Top*: Synthetic spectrum of the solar abundance model shown in Fig. 1. Observations (Charbonneau et al. 2008) are shown with $1-\sigma$ error-bars along with a 1450K black body (dotted line) and a model with no water opacity (in blue). *Bottom*: Standard model (red) compared to models without CO (blue) and CO mole fraction equal to 100 times that of the standard model. Diamonds are the band integrated model points at 4.5 μm .

detections relied on observations during primary transit, and thus relate to different regions of the planets than the secondary eclipse spectra (and photometry).

Interestingly, the *Spitzer* IRAC data (3.6 to 8 μm) for HD 189733 show evidence of H_2O and, to a lesser degree, CO absorption at the level predicted by model atmospheres (the mole fractions of CO and H_2O for the standard solar abundance model presented here are 6×10^{-4} and 5×10^{-4} respectively). The IRAC colors in particular are consistent with strong water absorption from ~ 4 to 8 μm . The good agreement between the no-redistribution model and the observations (Figs. 1 and 2) supports this interpretation. Furthermore, the IRS spectrum for HD 189733 reported to have no water absorption, is reasonably consistent with the model everywhere except at the blue and red edges (Fortney & Marley 2007). A flat ϵ_λ spectrum across 8 μm implies a very sharp rise in planet flux (see Fig. 2) that is inconsistent with the IRAC observations.

Spectra with different amounts of CO are compared to the observations in the lower panel of Fig. 2. An atmosphere absent of CO is excluded at roughly $2-\sigma$ and thus its presence is only tentatively suggested by the data. Unfortunately, the current precision of the 4.5 μm IRAC photometry is not sufficient to test large departures of Carbon from solar abundance or departures of CO from chemical equilibrium (Cooper & Showman 2006).

4. AN L-TYPE PLANET

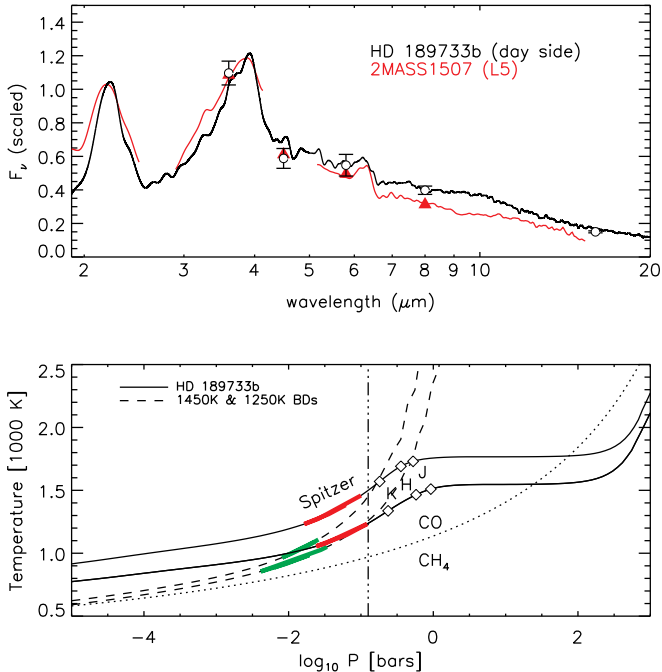


FIG. 3.— *Top*: The synthetic planet spectrum compared to a real IR spectrum of L5 brown dwarf 2MASS 1507. *Spitzer* photometry for HD 189733b and 2MASS 1507 are also shown, scaled to match at $3.6 \mu\text{m}$. *Bottom*: Temperatures and pressures for no-redistribution (top solid line) and full-redistribution (bottom solid line) models compared to 1250 and 1450K brown dwarf models (dashed lines). The *Spitzer* and near-IR photospheric depths are indicated by thick lines and filled symbols. The vertical dash-dotted line is the approximate boundary between efficient (higher P) and inefficient (lower P) horizontal circulation. The dotted curve denotes the region of equal CO/CH₄ equilibrium concentrations.

Many hot-Jupiters have day side photospheric temperatures and pressures comparable to those in L-type brown dwarfs and, despite potential differences in formation and evolution, a great deal can be learned by comparing observations of the former to observations of the latter. Figure 3 compares the HD 189733b observations and no-redistribution standard planet model to IRTF and *Spitzer* IR observations of an L5 brown dwarf, 2MASS 1507 (Cushing et al. 2006), each scaled to match at $3.6 \mu\text{m}$. The IRAC colors of the planet and brown dwarf are nearly identical. The decrease in flux across the shortest two IRAC bands is a hallmark of CO and H₂O absorption in brown dwarf atmospheres, lending support to the conclusions of the previous section. The observed IRS spectrum of the brown dwarf is also similar to the planet model spectrum, though a bit steeper. Also, the *Spitzer* photosphere in the brown dwarf is at lower pressures than in the planet where the two temperature structures have similar slopes and produce absorption features with similar relative depths.

The spectral similarities between HD 189733b and 2MASS 1507 answers an important question – this planet’s temperature structure can not be isothermal at the photospheric depths probed by *Spitzer*. This rules out one of the more plausible explanations for why the first set of IRS spectra showed no observed water ab-

sorption features. Looking back at Fig. 2, one can see that indeed the slope of the IRS planet spectrum, more or less, follows that of a black body and, by itself, is very suggestive of a purely isothermal structure. However, the $3.6 \mu\text{m}$ IRAC measurement, in concert with the longer wavelength data, rules out any single black body spectrum at several σ . Overall, the $> 3 \mu\text{m}$ spectral region of the planet appears to be remarkably similar to that of an L5 brown dwarf believed to have a solar atmospheric composition dominated by water and a steep temperature structure. However, as discussed below, irradiation driven atmospheric circulations most likely cause the short-wavelength spectrum to depart significantly from that of an L5 brown dwarf.

5. BALANCING THE BUDGET

Assuming HD 189733b is tidally locked, the incident stellar flux always enters the planet through the same hemisphere. This asymmetric heating may drive strong atmospheric circulations that transport significant amounts of energy to the night side (Showman & Guillot 2002; Cho et al. 2003). Determining the efficiency of energy redistribution across the day and night sides of a planet is, therefore, important for understanding the global atmospheric circulation. Recently Knutson et al. (2007) measured the night side flux to be $\sim 64\%$ of the day side flux at $8 \mu\text{m}$. This suggests that some fraction of the absorbed incident flux is, in fact, transported to the night side. How then can the day side *Spitzer* observations so closely match the predicted flux from a model with *zero* horizontal energy transport, as shown above?

After a few 100 Myrs, internal energy leftover from the formation of HD 189733b has mostly been lost, leaving the intrinsic luminosity $\sim 20,000$ times smaller than what the planet receives from the star. Thus, for old short-period planets like HD 189733b, the star is the primary energy source. Energy conservation requires that the planet’s atmosphere radiate as much energy as it receives and, if HD 189733b has a small albedo, the total luminosity one should expect from the planet is determined entirely by the stellar and orbital properties; $L_{\text{tot}} \sim 2.6 \times 10^{-5} L_{\odot}$. Consequently, the true *bolometric* luminosity of the planet’s day or night side (L_{day} or L_{night}) is needed to precisely determine the efficiency of redistribution. Note that the efficiency of redistribution is difficult to constrain with single band-pass photometry, since little leverage on the bolometric luminosity is obtained, even with a complete phase curve.

Fig. 4 shows νF_{ν} spectra for the full and no-redistribution planet models. Integrating the no-redistribution model spectrum (top curve) for $\lambda > 3.2 \mu\text{m}$ accounts for 33% of L_{tot} . Constraining L_{day} further requires measurements at shorter wavelengths. Fortunately, recent ground based observations have provided an upper limit for the day side *K*-band flux (less than 1.5 mJy) that helps complete the energy balance picture (Barnes et al. 2007). Though $\lambda_p^{\text{max}} \sim 3.6 \mu\text{m}$, the peak of the energy distribution sits at *K*-band making the *K*-band flux a very useful gauge of the short-wavelength fraction of L_{day} . By combining the day side measurements, one can safely conclude that a sizable fraction of the energy ($> 30\%$) is redistributed to the night side. Furthermore, these data tell us that a 1-D no-redistribution model over estimates the flux at *short*

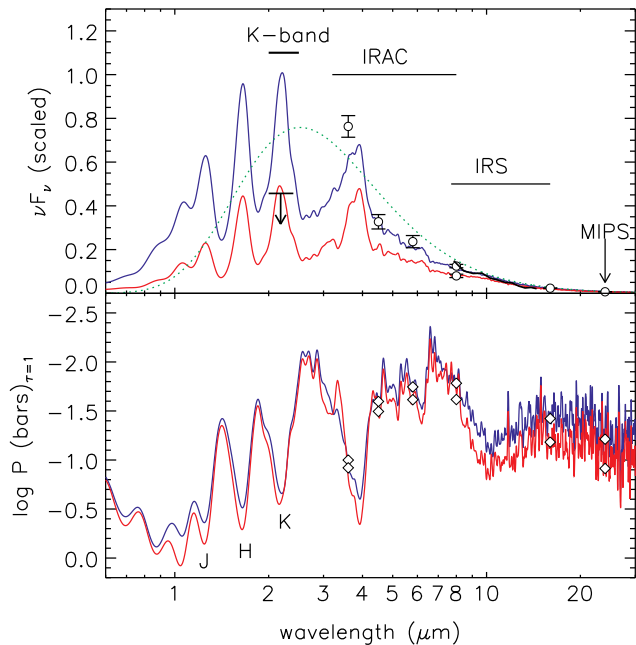


FIG. 4.— *Top*: planet energy distributions assuming full-redistribution (lower red line) and no-redistribution (top blue line) along with a 1450K blackbody spectrum. Over plotted are IR ground and space-based flux measurements for HD 189733b (see text for references). The lower point at 8 μm is the night side flux measurement from Knutson et al. (2007). *Bottom*: pressure at optical depth unity for both planet models. The location of the *Spitzer* and near-IR band-integrated pressures are labeled.

wavelengths ($< 2.5 \mu\text{m}$).

The estimate of energy redistributed can be further improved by using the Knutson et al. (2007) 8 μm night side measurement and the fact that only $\sim 66\%$ of L_{tot} remains to be shared across the entire night side spectrum and the day side spectrum not covered by *Spitzer*. The observed night side flux is close to the full-redistribution model spectrum shown in Fig. 4 suggesting that the night side *Spitzer* photospheric temperatures are close to those predicted by the full-redistribution model. Integrating this spectrum (slightly scaled down to match the 8 μm night side observation) across the complete wavelength range accounts for $\sim 43\%$ of L_{tot} , leaving $\sim 24\%$ of L_{tot} for the day side spectrum at $\lambda < 2.5 \mu\text{m}$. The day side *K*-band upper-limit is also close to the full-redistribution model spectrum suggesting that both day and night side near-IR spectra have similar flux levels.

As already discussed, the day side structure can not be entirely isothermal. The *Spitzer* data probe approximately the 0.1 to 0.01 bar region on the day side

while *J*, *H*, and *K*-bands probe higher pressures, > 100 mbars (see Fig. 4). Lower fluxes on the day side at short wavelengths (as indicated at *K*-band) compared to longer wavelengths suggests that energy redistribution is highly depth-dependent and occurs fairly deep in the atmosphere (> 0.1 bars). Similar depth-dependent redistribution has been explored for HD 209458b and is the expected behavior in many hot-Jupiters (Cooper & Showman 2005; Seager et al. 2005). Thus, the day and night sides probably have similar temperatures at $P > 0.1$ bars which are close to the full-redistribution structure shown in Fig. 3. The steady supply of incident flux from the star helps maintain the hot temperatures in the upper layers of the day side while on the night side temperatures at $P < 0.1$ bars are probably more similar to those of a cooler ($T_{\text{eff}} \sim 1250\text{K}$) brown dwarf structure (see Fig. 3). With lower temperatures, CH_4 begins to compete with CO as the dominant carbon bearing molecule on the night side, especially in the upper atmosphere. An important prediction of this scenario is that one should *not* expect significant phase variations at *J*, *H*, and *K*-band for this planet. Also, based on the models described here, the 24 μm night side flux is predicted to be $\sim 75\%$ of the day side flux, a prediction that will soon be tested by *Spitzer* observations. A more rigorous constraint on redistribution will require additional observations, especially of the night side, along with detailed global circulation models.

6. CONCLUSIONS

HD 189733b has an atmosphere rich in water and, most likely, CO. This planet's atmosphere also has day side temperatures, pressures, and chemical composition similar to a typical mid-L type brown dwarf. The fraction of energy redistributed from the day to night side has been estimated to be $\sim 43\%$ of the incident stellar flux. Furthermore, the bulk of the energy transport likely occurs at pressures higher than ~ 0.1 bars, indicating that the energy redistribution mechanism is most efficient at high pressures. It has also been demonstrated that the photospheric depths probed by *Spitzer* do not reach the isothermal layers predicted by atmosphere models. Consequently, an isothermal structure can *not* explain the flat ϵ_λ spectrum recently measured by IRS.

This paper benefited from the comments provided by the referee and many useful discussions with Adam Showman, Brad Hansen, and Jonathan Fortney. This research was supported by NASA through Origins of Solar Systems (NNX07AG68) and the *Spitzer* theoretical research grants to Lowell Observatory.

REFERENCES

- Barman, T. S., Hauschildt, P. H., & Allard, F. 2001, *ApJ*, 556, 885
- Barman, T. S., Hauschildt, P. H., & Allard, F. 2005, *ApJ*, 632, 1132
- Barman, T. 2007, *ApJ*, 661, L191
- Barnes, J. R., Barman, T. S., Prato, L., Segransan, D., Jones, H. R. A., Leigh, C. J., Collier Cameron, A., & Pinfield, D. J. 2007, *MNRAS*, 382, 473
- Bouchy et al. 2005, *A&A*, 444, L15
- Burrows, A., Sudarsky, D., & Hubeny, I. 2006, *ApJ*, 650, 1140
- Charbonneau et al. 2008, *ApJ*, submitted
- Cho, J. Y.-K., Menou, K., Hansen, B. M. S., & Seager, S. 2003, *ApJ*, 587, L117
- Cooper, C. S. & Showman, A. P. 2006, *ApJ*, 649, 1048
- Cooper, C. S. & Showman, A. P. 2005, *ApJ*, 629, L45
- Cushing et al. 2006, *ApJ*, 648, 614
- Deming, D., Harrington, J., Seager, S., & Richardson, L. J. 2006, *ApJ*, 644, 560
- Fortney, J. J. & Marley, M. S. 2007, *ApJ*, 666, L45
- Grillmair, C. J., Charbonneau, D., Burrows, A., Armus, L., Stauffer, J., Meadows, V., Van Cleve, J., & Levine, D. 2007, *ApJ*, 658, L115

- Knutson et al. 2007, *Nature*, 447, 183
Richardson, L. J., Deming, D., Horning, K., Seager, S., & Harrington, J. 2007, *Nature*, 445, 892
Seager, S., Richardson, L. J., Hansen, B. M. S., Menou, K., Cho, J. Y.-K., & Deming, D. 2005, *ApJ*, 632, 1122
Showman, A. P. & Guillot, T. 2002, *A&A*, 385, 166
Tinetti et al. 2007, *Nature*, 448, 169